

## Supplement

### Part 1: Free energy profile calculations

Free energy profile of each amine accumulated onto Kao surface is calculated with weighted histogram analysis method<sup>1</sup> based on umbrella sampling from MD trajectory of each amine. Herein, Kao( $\text{Al}_2\text{Si}_2\text{O}_5(\text{OH})_4$ ) bulk is made up of an  $\text{AlO}_6$  octahedral sheet and a  $\text{SiO}_4$  tetrahedral sheet<sup>2</sup>. (001) surface of Kao containing 1530 atoms is constructed in the box of  $26.0 \times 26.9 \times 22.1 \text{ \AA}^3$ . A vacuum layer of  $30 \text{ \AA}$  is added above equilibrated Kao surface along the Z-direction to avoid the interferences from circumambient mirror images. Single amine molecule is placed above  $20 \text{ \AA}$  from the mass center of Kao. Configurations of amine-Kao are further equilibrated in *NVT*-MD for 500 ps. To investigate heterogeneous uptake process from air onto Kao surface, each amine molecule is moved by a step of  $1.0 \text{ \AA}$ . At the updated position of amine molecule in each window, amine-Kao system is re-equilibrated within 250 ps and subsequently sampled within another 250 ps in *NVT* ensemble at 1 fs timestep. 21 windows are set to describe transport path of amine molecule from air to the mass center of Kao surface. Based on the MD results of each window, free energy profile of amine-Kao molecule is calculated by the umbrella sampling<sup>3</sup> and weighted with the histogram analysis method.<sup>1,4</sup> The bias potential force constant is equal to  $10 \text{ kcal} \cdot \text{mol}^{-1}$ .<sup>5,6</sup> The final free energy profile is shown in Fig. S1A. The structure of amine-Kao with the lowest free energy indicates the adsorption site of amines on Kao surface.

### Part 2: Simple forcing efficiency

Simple forcing efficiency (SFE) proposed by Bond and Bergstrom<sup>7</sup> is calculated to quantify the influence of heterogeneous oxidation mechanisms on RFE of amine-Kao mixed particle. SFE is obtained from formula (1):

$$\text{SFE} = \frac{S_0}{4} \tau_{\text{atm}}^2 (1 - F_c) [2(1 - a_s)^2 \beta \cdot \text{MSC} - 4a_s \cdot \text{MAC}] \quad (1)$$

where  $S_0$  is solar irradiance,  $\tau_{\text{atm}}$  is atmospheric transmittance,  $F_c$  is cloud fraction,  $a_s$  is surface albedo,  $\beta$  is backscattering coefficient. Under the same atmospheric conditions,  $S_0$ ,  $\tau_{\text{atm}}$ ,  $F_c$ ,  $a_s$  and  $\beta$  keep constant. MSC and MAC are scattering and absorption cross section area per unit

mass of mixed particles, respectively. Thereinto, the relationship between  $p$  and MAC is described as<sup>8</sup>:

$$30 \quad p = \frac{\rho \lambda \text{MAC}(\lambda)}{4\pi} \quad (2)$$

where  $\rho$  and  $\lambda$  is the particle density and the wavelength of light, respectively. Herein, all the values of  $p$  for initial and oxidized amine-Kao particles are smaller than 0.002, which can be ignored. MAC is thus estimated to be zero. Therefore, light adsorption of amine-Kao mixed particle is not considered in evaluating RFE.

35 The relationship between  $n$  and MSC is determined by formula (3)<sup>7</sup>:

$$\text{MSC} = \frac{4\pi^4 d^3 V}{M\lambda} \left( \frac{n^2 - 1}{n^2 + 2} \right)^2 \quad (3)$$

where  $d$ ,  $V$ , and  $M$  is the diameter, volume and  $M$  of amine-Kao particle, and  $\lambda$  is the wavelength of light.

To roughly estimate changes in SFE resulted from increased  $n$ ,  $\Delta\text{SFE}$  is defined as the ratio of SFE of amine-Kao particle to that of Kao. Note the changes in mass, volume and diameter changes of particles during oxidation process are not considered. Therefore, which is described as follows:

$$40 \quad \Delta\text{SFE} = \frac{\text{SFE}_{\text{amine-Kao}} - \text{SFE}_{\text{initial}}}{\text{SFE}_{\text{Kao}}} = \frac{\text{MSC}_{\text{amine-Kao}}}{\text{MSC}_{\text{Kao}}} - 1 = \frac{\left( \frac{n_{\text{amine-Kao}}^2 - 1}{n_{\text{amine-Kao}}^2 + 2} \right)^2}{\left( \frac{n_{\text{Kao}}^2 - 1}{n_{\text{Kao}}^2 + 2} \right)^2} - 1 \quad (4)$$

### Part 3: Figures and tables of SI.

**Table. S1.** Summarized  $\Delta E^\ddagger$ ,  $\Delta E_r$  and  $k$  values for each reaction step of amine at 298 K. For energy barrier reaction,  $ki$  is calculated based on  $\Delta E^\ddagger$ , and for energy barrierless reactions,  $ki$  is calculated based on  $\Delta E_r$ .

No.	Reaction	$T$ (K)	$\Delta E^\ddagger$ (kcal/mol)	$\Delta E_r$ (kcal/mol)	$ki$	Unit of $k$
R1	MA+·OH→MA·Rc+H <sub>2</sub> O	298	-15.09	-22.50	1.27×10 <sup>5</sup>	s <sup>-1</sup> molec <sup>-1</sup> cm <sup>3</sup>
R2	DMA+·OH→DMA·Rc+H <sub>2</sub> O	298	-9.42	-23.33	9.22	s <sup>-1</sup> molec <sup>-1</sup> cm <sup>3</sup>
R3	TMA+·OH→TMA·Rc+H <sub>2</sub> O	298	2.75	-19.16	1.65×10 <sup>-8</sup>	s <sup>-1</sup> molec <sup>-1</sup> cm <sup>3</sup>
R4	MA+·OH→MA·R <sub>N</sub> +H <sub>2</sub> O	298	-6.96	-13.42	1.24×10 <sup>-1</sup>	s <sup>-1</sup> molec <sup>-1</sup> cm <sup>3</sup>
R5	DMA+·OH→DMA·R <sub>N</sub> +H <sub>2</sub> O	298	-6.26	-15.60	1.54×10 <sup>-2</sup>	s <sup>-1</sup> molec <sup>-1</sup> cm <sup>3</sup>
R6	MA-Rc+O <sub>2</sub> →MA-RO <sub>2</sub> ·	298	/	-15.71	8.24×10 <sup>4</sup>	s <sup>-1</sup> molec <sup>-1</sup> cm <sup>3</sup>
R7	DMA-Rc+O <sub>2</sub> →DMA-RO <sub>2</sub> ·	298	/	-17.90	3.32×10 <sup>6</sup>	s <sup>-1</sup> molec <sup>-1</sup> cm <sup>3</sup>
R8	TMA-Rc+O <sub>2</sub> →TMA-RO <sub>2</sub> ·	298	/	-15.47	5.51×10 <sup>4</sup>	s <sup>-1</sup> molec <sup>-1</sup> cm <sup>3</sup>
R9	MA-RO <sub>2</sub> ·+NO→MA-RO·+NO <sub>2</sub>	298	/	-4.70	7.08×10 <sup>-4</sup>	s <sup>-1</sup> molec <sup>-1</sup> cm <sup>3</sup>
R10	DMA-RO <sub>2</sub> ·+NO→DMA-RO·+NO <sub>2</sub>	298	/	-33.91	1.79×10 <sup>18</sup>	s <sup>-1</sup> molec <sup>-1</sup> cm <sup>3</sup>
R11	TMA-RO <sub>2</sub> ·+NO→TMA-RO·+NO <sub>2</sub>	298	/	-26.51	6.75×10 <sup>12</sup>	s <sup>-1</sup> molec <sup>-1</sup> cm <sup>3</sup>
R12	MA-RO·+O <sub>2</sub> →NH <sub>2</sub> CHO+HO <sub>2</sub>	298	3.17	-58.74	4.30×10 <sup>-9</sup>	s <sup>-1</sup> molec <sup>-1</sup> cm <sup>3</sup>
R13	DMA-RO·+O <sub>2</sub> →CH <sub>3</sub> NHNHO+HO <sub>2</sub>	298	4.91	-55.58	3.28×10 <sup>-10</sup>	s <sup>-1</sup> molec <sup>-1</sup> cm <sup>3</sup>
R14	TMA-RO·+O <sub>2</sub> →(CH <sub>3</sub> ) <sub>2</sub> NCHO+HO <sub>2</sub>	298	3.22	-60.39	3.32×10 <sup>-9</sup>	s <sup>-1</sup> molec <sup>-1</sup> cm <sup>3</sup>

R15	MA-RO <sub>2</sub> · → HN=CH <sub>2</sub> +HO <sub>2</sub>	298	27.38	16.08	3.33×10 <sup>-7</sup>	s <sup>-1</sup>
R16	DMA-RO <sub>2</sub> · → CH <sub>3</sub> N=CH <sub>2</sub> +HO <sub>2</sub>	298	21.16	7.54	4.98×10 <sup>-3</sup>	s <sup>-1</sup>
R17	MA-RO <sub>2</sub> · → ·NHCH <sub>2</sub> OOH (IM17)	298	27.38	16.08	1.34×10 <sup>-7</sup>	s <sup>-1</sup>
R18	DMA-RO <sub>2</sub> · → ·CH <sub>2</sub> NHCH <sub>2</sub> OOH(IM18)	298	19.61	13.66	1.85×10 <sup>-1</sup>	s <sup>-1</sup>
R19	TMA-RO <sub>2</sub> · → ·CH <sub>2</sub> N(CH <sub>3</sub> )CH <sub>2</sub> OOH(IM19)	298	14.15	9.47	2.23×10 <sup>3</sup>	s <sup>-1</sup>
R20	·NHCH <sub>2</sub> OOH+O <sub>2</sub> (RC20) → NH=CHOOH+HO <sub>2</sub> (Pro20)	298	5.79	-47.65	8.42×10 <sup>-11</sup>	s <sup>-1</sup> molec <sup>-1</sup> cm <sup>3</sup>
R21	·CH <sub>2</sub> NHCH <sub>2</sub> OOH+O <sub>2</sub> (RC21) → ·OOCH <sub>2</sub> NHCH <sub>2</sub> OOH(IM21)	298	/	-31.73	4.51×10 <sup>16</sup>	s <sup>-1</sup> molec <sup>-1</sup> cm <sup>3</sup>
R22	·CH <sub>2</sub> N(CH <sub>3</sub> )CH <sub>2</sub> OOH+O <sub>2</sub> (RC22) → ·OOCH <sub>2</sub> N(CH <sub>3</sub> )CH <sub>2</sub> OOH(IM22)	298	/	-14.49	1.05×10 <sup>4</sup>	s <sup>-1</sup> molec <sup>-1</sup> cm <sup>3</sup>
R23	·OOCH <sub>2</sub> NHCH <sub>2</sub> OOH(IM21) → HOOCH <sub>2</sub> NHCHO+·OH	298	33.50	-41.69	1.00×10 <sup>-11</sup>	s <sup>-1</sup>
R24	·OOCH <sub>2</sub> N(CH <sub>3</sub> )CH <sub>2</sub> OOH(IM22) → HOOCH <sub>2</sub> N(CH <sub>2</sub> ·)CH <sub>2</sub> OOH(IM24)	298	12.93	7.71	1.72×10 <sup>4</sup>	s <sup>-1</sup>
R25	HOOCH <sub>2</sub> N(CH <sub>2</sub> ·)CH <sub>2</sub> OOH+O <sub>2</sub> (RC25) → HOOCH <sub>2</sub> N(CH <sub>2</sub> OO·)CH <sub>2</sub> OOH(IM25)	298	/	-22.15	4.32×10 <sup>9</sup>	s <sup>-1</sup> molec <sup>-1</sup> cm <sup>3</sup>
R26	HOOCH <sub>2</sub> N(CH <sub>2</sub> OO·)CH <sub>2</sub> OOH(IM25) → (HOOCH <sub>2</sub> ) <sub>2</sub> NCHO+·OH	298	9.38	-52.18	4.20×10 <sup>6</sup>	s <sup>-1</sup>

The rate constant for the reaction step with  $\Delta E^\ddagger = 20$  kcal/mol is  $1.38 \times 10^{-2} \text{ s}^{-1}$  (the first order reaction) and  $5.68 \times 10^{-22} \text{ s}^{-1} \text{ molec}^{-1} \text{ cm}^3$  (the second order reaction).

**Table. S2.** Comparisons of  $\Delta E^\ddagger$  and  $k_i$  between homogeneous and heterogeneous oxidation reactions of MA, DMA and TMA.

Amine	No.	Heterogeneous oxidation (this work)		Homogeneous oxidation		Reference
		$\Delta E^\ddagger$ (kcal/mol)	$k_i$	$\Delta E^\ddagger$ (kcal/mol)	$k_i$	
MA	R1	-15.09	$1.27 \times 10^5 \text{ s}^{-1} \text{ molec}^{-1} \text{ cm}^3$	6.16(C-H)	$1.88 \times 10^{-11} \text{ s}^{-1} \text{ molec}^{-1} \text{ cm}^3$	<sup>9</sup>
	R12	3.17	$4.30 \times 10^{-9} \text{ s}^{-1} \text{ molec}^{-1} \text{ cm}^3$	/	/	
DMA	R2	-9.42	$9.22 \text{ s}^{-1} \text{ molec}^{-1} \text{ cm}^3$	8.46	$6.39 \times 10^{-11} \text{ s}^{-1} \text{ molec}^{-1} \text{ cm}^3$	<sup>9</sup>
	R13	4.91	$3.28 \times 10^{-10} \text{ s}^{-1} \text{ molec}^{-1} \text{ cm}^3$	/	/	
TMA	R3	2.75	$1.65 \times 10^{-8} \text{ s}^{-1} \text{ molec}^{-1} \text{ cm}^3$	8.23	$5.73 \times 10^{-11} \text{ s}^{-1} \text{ molec}^{-1} \text{ cm}^3$	<sup>9</sup>
	R14	3.22	$3.32 \times 10^{-9} \text{ s}^{-1} \text{ molec}^{-1} \text{ cm}^3$	/	/	
	R19	14.15	$2.23 \times 10^3 \text{ s}^{-1}$	17.8/16	$2.9 \text{ s}^{-1}$	<sup>10, 11</sup>
	R24	12.93	$1.72 \times 10^4 \text{ s}^{-1}$	18.2/18.4	$0.52 \text{ s}^{-1}$	<sup>10, 11</sup>
	R26	9.38	$4.20 \times 10^6 \text{ s}^{-1}$	20.1/18.1	$5.1 \times 10^{-2} \text{ s}^{-1}$	<sup>10, 11</sup>

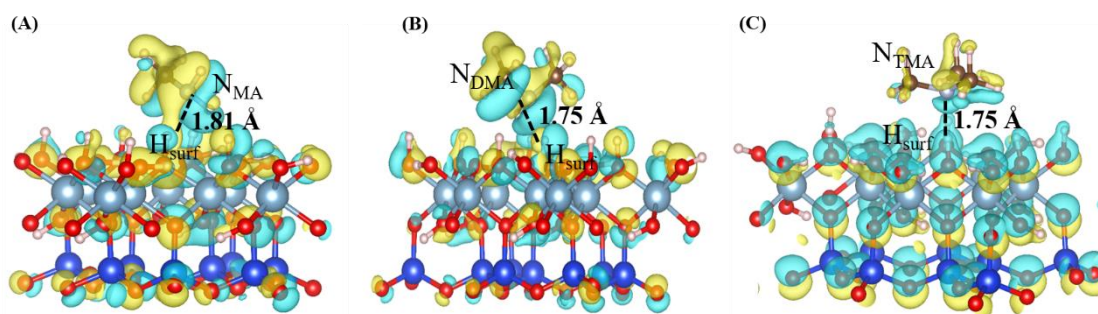


**Fig. S1.** Charge density differences and desorption energies of (A) MA-Kao, (B) DMA-Kao and (C) TMA-Kao mixed particles, respectively. Yellow and blue regions mean the regions where electron density increases and decreases, respectively.

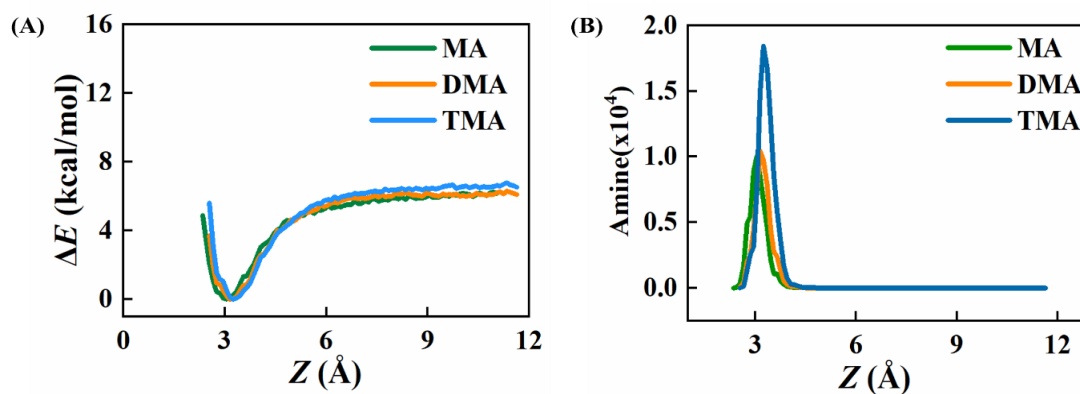


**Fig. S2.** Amine uptake by Kao particle simulated by classic MD simulation. (A) Free-energy profiles and (B) relative concentration changes of three amines accumulated on Kao surface.

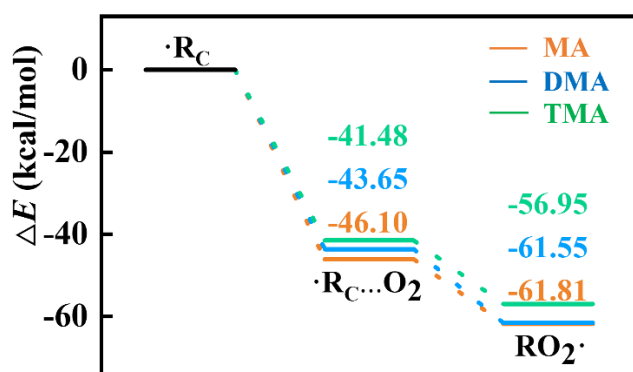


**Fig. S3.** PES of  $R_C \cdot$  conversion into  $RO_2 \cdot$  on Kao surface.

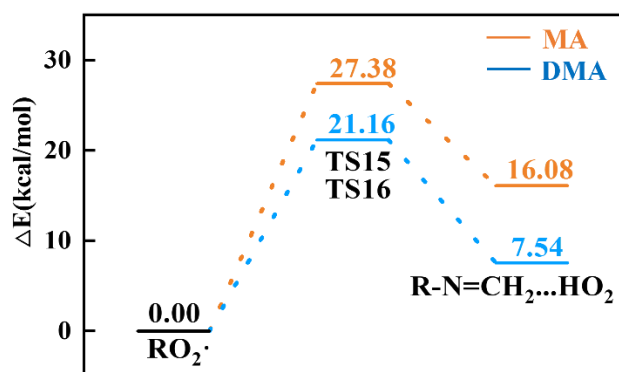


**Fig. S4.** PES of the H-abstraction reactions of MA's and DMA's  $\text{RO}_2\cdot$  under clean condition.

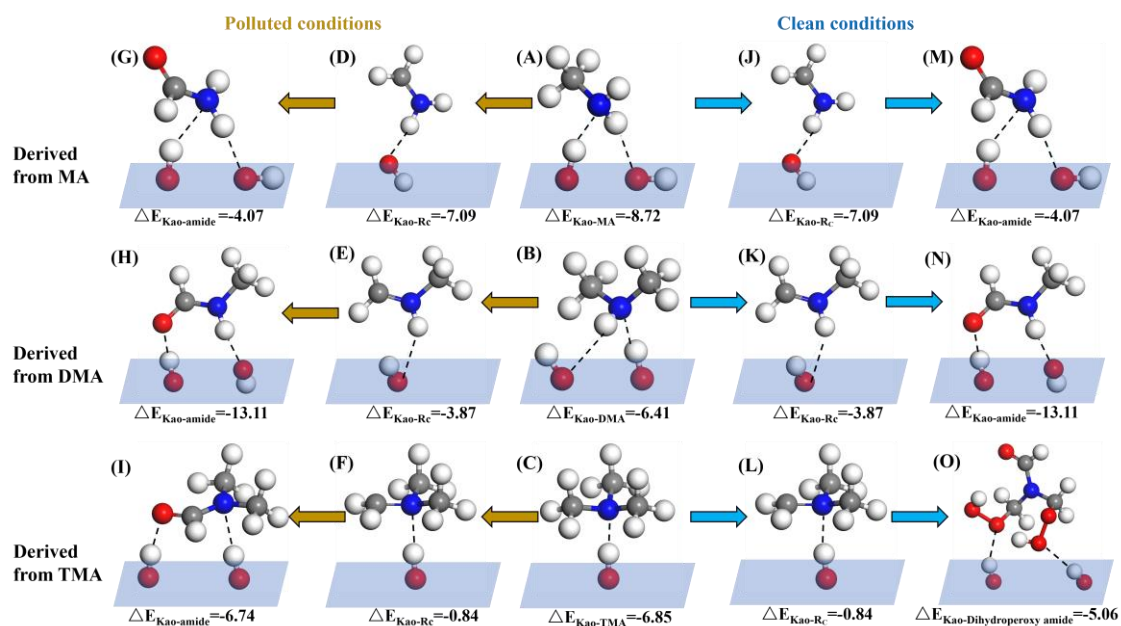


**Fig. S5.** All configurations and corresponding desorption energies of different amines and their oxidant products under polluted (brown arrows) and clean (blue arrows) conditions. (unit: kcal/mol)

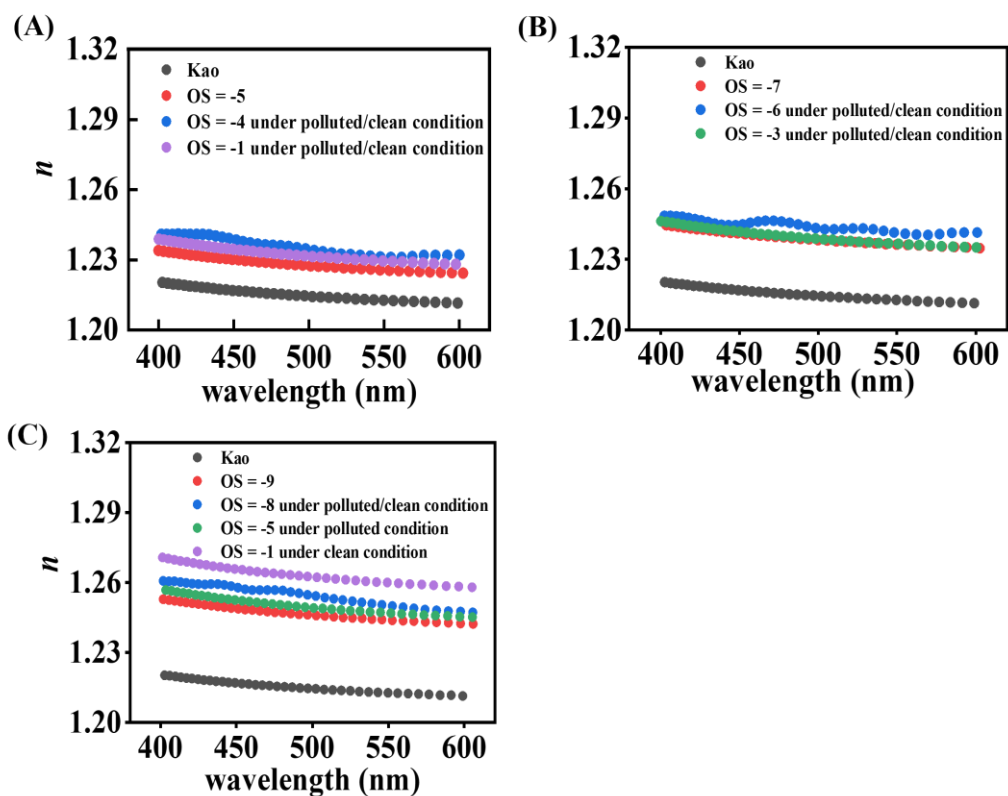


**Fig. S6.**  $n$  changes of each amine-Kao particle with increased wavelength (400 – 600 nm) under polluted and clean conditions. Results for (A) MA-Kao, (B) DMA-Kao or (C) TMA-Kao particles, respectively.



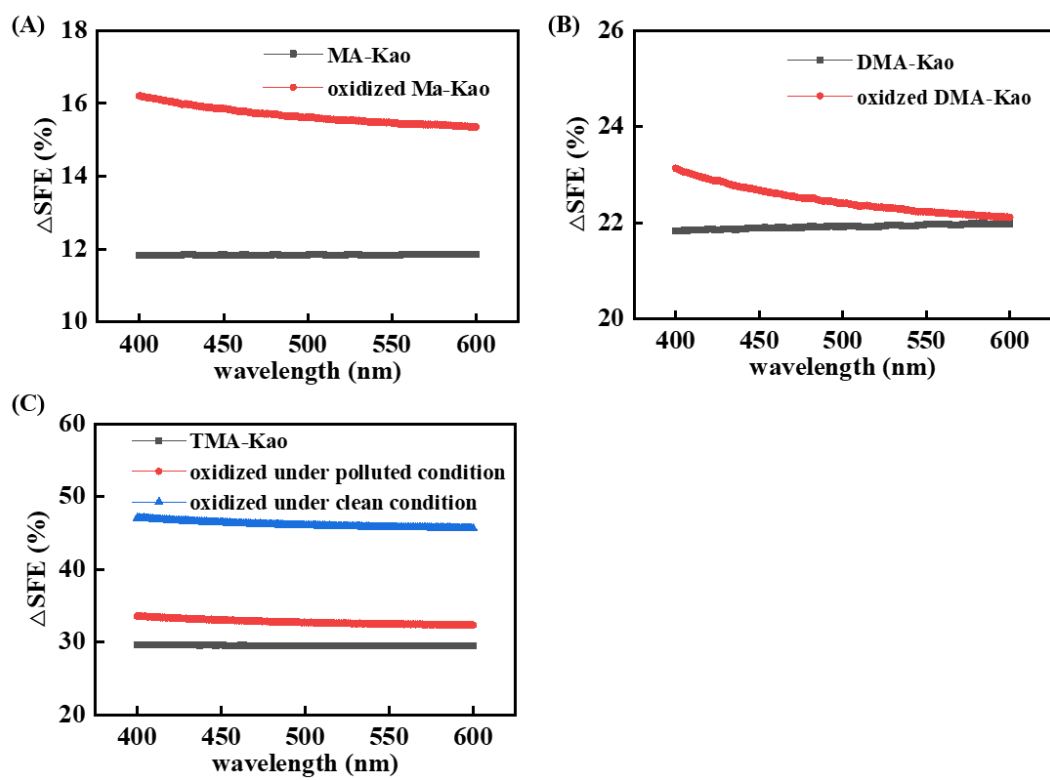


**Fig. S7.**  $\Delta$ SFE profile of initial and oxidized (A) MA-Kao, (B) DMA-Kao and (C) TMA-Kao particles with increased wavelengths.

## References in SI

1. Kumar, S.; Rosenberg, J. M.; Bouzida, D.; Swendsen, R. H.; Kollman, P., Multidimensional free-energy calculations using the weighted histogram analysis method. *J. Comput. Chem* **1995**, *16*, 1339-1350.
2. Tenney, C. M.; Cygan, R. T., Molecular Simulation of Carbon Dioxide, Brine, and Clay Mineral Interactions and Determination of Contact Angles. *Environmental Science & Technology* **2014**, *48*, (3), 2035-2042.
3. Torrie, G. M.; Valleau, J. P., Nonphysical sampling distributions in Monte Carlo free-energy estimation: Umbrella sampling. *J. Comput. Phys.* **1997**, *23*, 187.
4. Roux, B., The calculation of the potential of mean force using computer simulations. *Comput. Phys. Comm.* **1995**, *91*, 275-282.
5. Martins-Costa, M. T. C.; García-Prietoa, F. F.; Ruiz-López, M. F., Reactivity of aldehydes at the air–water interface. Insights from molecular dynamics simulations and ab initio calculations. *Org. Biomol. Chem.* **2015**, *13*, 1673.
6. Martins-Costa, M. T. C.; Anglada, J. M.; Francisco, J. S.; Ruiz-Lopez, M. F., Reactivity of Volatile Organic Compounds at the Surface of a Water Droplet. *J. Am. Chem. Soc.* **2012**, *134*, (28), 11821-11827.
7. Bond, T. C.; Bergstrom, R. W., Light Absorption by Carbonaceous Particles: An Investigative Review. *Aerosol Science and Technology* **2007**, *40*, (1), 27-67.
8. Yang, Z.; Tsona, N. T.; George, C.; Du, L., Nitrogen-Containing Compounds Enhance Light Absorption of Aromatic-Derived Brown Carbon. *Environ Sci Technol* **2022**, *56*, (7), 4005-4016.
9. Onel, L.; Thonger, L.; Blitz, M. A.; Seakins, P. W.; Bunkan, A. J.; Solimannejad, M.; Nielsen, C. J., Gas-phase reactions of OH with methyl amines in the presence or absence of molecular oxygen. An experimental and theoretical study. *J Phys Chem A* **2013**, *117*, (41), 10736-45.
10. Ma, F.; Xie, H. B.; Li, M.; Wang, S.; Zhang, R.; Chen, J., Autoxidation mechanism for atmospheric oxidation of tertiary amines: Implications for secondary organic aerosol formation. *Chemosphere* **2021**, *273*, 129207.
11. Moller, K. H.; Berndt, T.; Kjaergaard, H. G., Atmospheric Autoxidation of Amines. *Environ Sci Technol* **2020**, *54*, (18), 11087-11099.